From Classical to Quantum Glasses with Ultracold Polar Molecules

Wolfgang Lechner* and Peter Zoller

Institute for Quantum Optics and Quantum Information, Austrian Academy of Sciences, 6020 Innsbruck, Austria and Institute for Theoretical Physics, University of Innsbruck, 6020 Innsbruck, Austria

(Received 7 August 2013; published 30 October 2013)

We study the dynamics of a bilayer system of ultracold polar molecules, which exhibits classical and quantum glassy behavior, characterized by long tails in the relaxation time and dynamical heterogeneity. In the proposed setup, quantum fluctuations are of the order of thermal fluctuations and the degree of frustration can be tuned by the interlayer distance. We discuss the possible observation of a glassy anomalous diffusion and dynamical heterogeneity in experiment using internal degrees of freedom of the molecules in combination with optical detection.

DOI: 10.1103/PhysRevLett.111.185306 PACS numbers: 67.85.−d, 64.70.P−

The recent experimental realization of cold ensembles of polar molecules [1] has opened a new pathway to explore the dynamics of quantum many-body systems with strong, long-range, and anisotropic polar interactions [2–9]. In combination with low-dimensional trapping geometries, this allows the realization of stable many-body phases, for example, in the form of 1D wires or 2D pancakes [10–13], or as stacked pancakes representing coupled multilayer systems [14–18]. Most of the experimental and theoretical studies of polar molecular gases have focused thus far on the quantum degenerate regime, and on equilibrium phenomena, including superfluid and crystal phases, quantum magnetism, and topological phases (for a review, see [8,9]). Instead, our interest below will be on nonequilibrium many-body dynamics. We will show that a bilayer setup of ultracold polar bosonic molecules can feature a *glass phase*, and we present methods to prepare this phase and measure the relevant order parameters with tools available with present experimental setups. The unique feature and the theoretical challenge of glass physics with cold molecular ensembles is the possibility to study the crossover from classical to quantum glasses.

A glass phase is characterized by a plateau in the relaxation time scale, known as *aging*, with exponentially increasing tails that prevent the system from reaching its equilibrium state [13,19–21]. In a structural glass, global reorganization to the equilibrium is prevented from geometric frustration as a result of the dynamics [22]. While large reorientation is slow, on a local scale, relaxation can be fast, a phenomenon known as *dynamical heterogeneity* [23]. In a classical glass this relaxation dynamics is dominated by thermal fluctuations, and a considerable understanding of the glass transition has been gained from various theoretical methods [19,24–28] and experimental model systems [29–31]. In contrast, the question of the influence of quantum fluctuations on the glass relaxation dynamics is far less well understood. Recent theoretical studies indicate, based on analytical [28,32,33] and numerical [34–36] methods, that quantum fluctuations can enhance but also inhibit the glass transition.

In this Letter, we propose and analyze a protocol to prepare and measure a glass phase in a bilayer setup of cold polar molecules in the regime of the crossover from a classical to a quantum glass. We assume ultracold molecules prepared in their electronic and rovibrational ground states, where a static electric field $\mathbf{E} \equiv E\mathbf{e}_z$ oriented perpendicular to the trapping layers in the xy plane induces an electric dipole moment $\mathbf{d} \equiv d\mathbf{e}_z$. Thus the molecules will interact according to strong, long-range, and anisotropic dipole-dipole interaction. The stacked pancake potential of Figs. 1(a) and 1(b) can be realized with a 1D optical lattice with layer separation s controllable by laser parameters. For strong confinement the motion of the molecule within each layer can be described as an effective 2D dynamics, while the tunneling between adjacent layers will be suppressed by a sufficiently high barrier. The Hamiltonian for our bilayer system thus has the form $H = H_A + H_B + H_{AB}$. Here, H_A (H_B) is the Hamiltonian for the intralayer dynamics,

$$H_X = \sum_{i\in X}\left(\frac{\mathbf{p}_i^2}{2m} + V_T(\mathbf{r}_i)\right) + \sum_{i,j\in X}\frac{d_X^2}{4\pi\epsilon_0}\frac{1}{r_{ij}^3} \qquad (X = A, B), \tag{1}$$

as the sum of kinetic energy and a transverse trapping potential, and the (purely repulsive) dipolar interaction with in-plane distance r. The interlayer interactions are

$$H_{AB} = \sum_{i\in A, j\in B}\frac{d_A d_B}{4\pi\epsilon_0}\frac{1}{R_{ij}^3}\left(1 - \frac{3s^2}{R_{ij}^2}\right), \tag{2}$$

with s the layer separation and R the distance between the molecules with $R^2 = r^2 + s^2$. Note that our model allows for different dipole moments d_A and d_B in layers A and B, respectively. Different effective dipole moments in the two layers can be achieved, e.g., by a gradient in the electric field E_z or by engineering of the interactions using internal

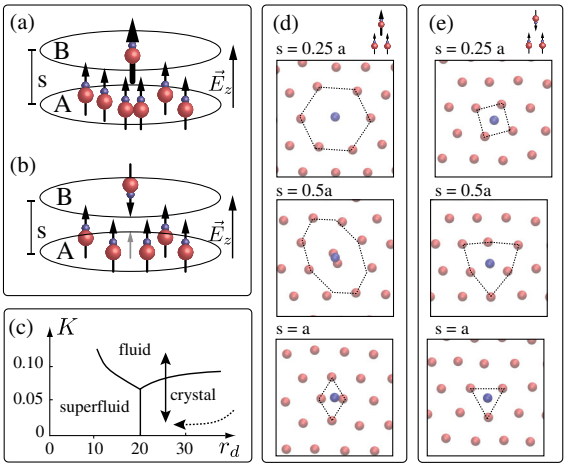

FIG. 1 (color online). Bilayer setup of trapped polar molecules with parallel dipole moments (a) and antiparallel dipole moments (b). The lower layer represents a high density dipolar crystal, the upper layer is loaded with low density (see text). A typical route to enter the glass phase is to quench the system from the liquid to a supercooled phase. In contrast, here the glass phase is reached by decreasing the layer separation s. (c) Sketch of the phase diagram of a single layer of bosonic polar molecules with the ratio between kinetic energy and interaction K and r_d from Ref. [10]. Note that the limit $m \to \infty$ corresponds to the classical limit as the extension of the wave function vanishes with $\lambda_{dB} = h/(2\pi m k_B T)^{1/2}$. The arrow indicates the parameter region of interest. (d) For parallel dipoles [(a)], the effective volume and symmetry of the defects depends on the interlayer separation. The ground state from a classical simulated annealing calculation at $T = 0$ includes patterns of triangular and cubic symmetries where particles in the crystal layer (red) are displaced by the molecules in the defect layer (blue). (e) For antiparallel dipoles [(b)], defect patterns can range from triangular, cubic to fivefold symmetries.

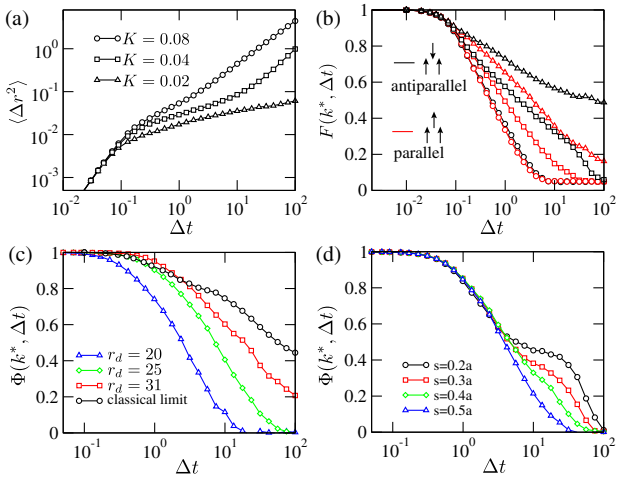

FIG. 2 (color online). Glass order parameters in the classical (top) and semiclassical regime from path integral calculations (bottom). (a) In the glass phase, the average mean squared displacement of the particles deviates from the constant diffusion. In the antiparallel setup the plateau extends over the whole sampling time below $K < 0.02$ of the combined system. (b) The relaxation of the time dependent structure factor $F(k^*, t)$ for $s = 0.5a$ with $d_B = 4d_A$ (black) and $d_B = -d_A$ (red) diverges when approaching the glass phase [symbols as in (a)]. (c) Relaxation dynamics with initial temperature $K = 0.01$ in the antiparallel setup for various choices for $r_d = Dm/[\hbar^2\langle a \rangle]$ of the combined system, with $\langle a \rangle$ the average distance in the xy plane. Parameters are chosen such that the system enters the glass phase in the classical limit $m \to \infty$ and melts with smaller r_d due to quantum fluctuations (blue). This allows one to study the crossover from a classical glass to a quantum phase. (d) Relaxation dynamics as a function of the layer separation with effective $r_d \approx 20$–25 and $K = 0.02$ in the antiparallel setup. While for distance $s = 0.5a$ the system is a liquid due to large quantum fluctuations (blue), one reaches the glass phase when approaching $s = 0.2a$ (black).

rotational degrees of freedom [8]. As we will see below, this feature is essential to observe clear signatures of a glass phase.

The basic steps of our protocol to study glassy dynamics are as follows. (i) We start with two uncoupled layers (s large), where layer A is in a high density 2D crystal phase and layer B is in a low density gas phase. To prepare the initial state for the dynamics, the layer separation is quenched to a small distance s, which leads to the formation of defects with various symmetries and patterns depending on the value of s (see Fig. 1). (ii) We evolve the system to find glassy dynamics, identified by dynamical heterogeneity, the deviation from the linear diffusion law, and a plateau in the relaxation (see Fig. 2). (iii) In order to measure these features in a possible experiment with cold molecules, we introduce *marker molecules*, i.e., molecules prepared in a different internal state, which allow tracking the time evolution of the particles (see Fig. 3).

Preparation of the initial state.—We first prepare molecules in two uncoupled layers: a dipolar crystal of polar molecules in layer A and a low density phase of defects in layer B. For uncoupled layers, the phase of layer A is described by parameters $r_d = Dm/[\hbar^2 a]$ and $K = k_B T a^3/D$, where $D = d_A^2/(4\pi\epsilon_0)$. The first parameter is the ratio of the dipolar interaction D/a^3 for a given mean intralayer distance between the particles a and the kinetic energy $\hbar^2/ma^2$, which in the dipolar crystal phase is $r_d \gg 1$. The second parameter measures the temperature in units of the interaction. For bosons the relevant phase diagram is sketched in Fig. 1(c) [10], which at low temperatures shows a low density (2D) superfluid phase, a high density crystal phase, and a high temperature fluid phase. The theoretically predicted conditions for the formation of a self-assembled crystal are, in the case of bosons, $r_d > 20$ and $K < 0.1$ [10]. We note that these conditions for r_d and K are a requirement for temperature, density, and dipole moment. While in present experiments with KRb the crystalline phase has not been realized, the ongoing effort in the laboratory to prepare cold ensembles of LiCs molecules [37] with its large electric dipole moment $\mu = 5.3$ D and mass $m = 92$ u provides a promising candidate to obtain

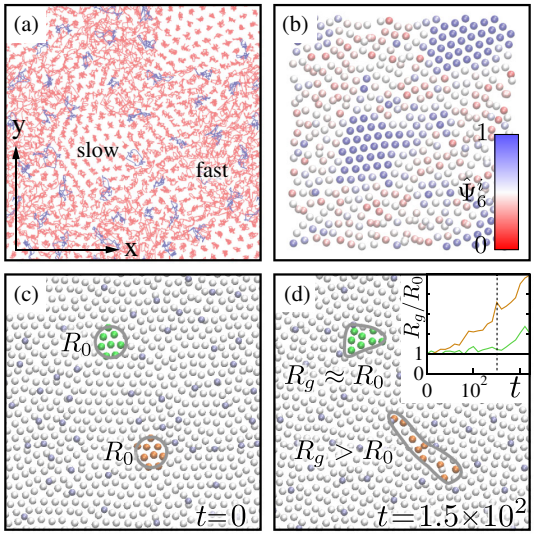

FIG. 3 (color online). Dynamical heterogeneity of a quantum glass in the proposed setup. Molecules in an excited internal state act as marker molecules to identify glassy dynamics. (a) Typical initial configuration of layer A (red) and layer B (blue) depicted as the projection of the paths onto real space. (b) The parameter ψ_6^i measures the relative order in the vicinity of particle i (see Supplemental Material [38]). Here, regions of large (small) order are regions of small (large) classical diffusion and a small (large) extension of the particle wave function. (c) Snapshots of two possible initial choices of marker molecule positions (green and orange) at $\Delta t = 0$ with $R_g = R_0$. The particle positions indicated by spheres represent the maximum of the path probability in layer A (gray) and layer B (light blue). (d) Indicating dynamical heterogeneity, the radius of gyration of marker molecules after time $\Delta t = 1.5 \times 10^2$ differs depending on the initial position. The cloud of marker molecules placed in an inactive region (green) of the glass follows the dynamics of an amorphous crystal $R_g = R_0$ while molecules in a mobile region (orange) show a fast increase in size (inset). Note that dynamical heterogeneity is a general feature of glasses, which is also present in systems without apparent partial crystallinity (see Supplemental Material [38]).

dipolar crystals. In this case for a given temperature $T = 0.1$ μK the requirement on r_d and K corresponds to an effective (induced) dipole moment of $d_A = 2.17$ D and a lattice spacing of the self-assembled triangular crystal $a = 0.32$ μm. We assume that the density in layer B is lower than that in layer A while all other parameters are the same. In the following we find it convenient to define length, energy, and time in the reduced units a, D/a^3, $a\sqrt{ma^3/D}$, respectively.

To prepare the initial state for the glassy dynamics, the two layers are brought together by a quench in the layer separation. The speed of the quench is chosen such that nonadiabatic effects are negligible [38]. We consider two cases: the dipoles can be aligned parallel [see Fig. 1(a)] or antiparallel [see Fig. 1(b)]. Figure 1(d) depicts the resulting defect patterns for parallel dipoles $d_B = 4d_A$ where molecules belonging to different layers attract each other. This attraction leads to stable dimers or trimers [8] if the two layers are separated by $s \leq a$. These composite defects are reminiscent of interstitials in a crystal. Here, the effective volume of the interstitials can be tuned by the ratio of the dipole moments d_A/d_B and the interlayer separation s. For various layer separations ranging from $s = 0.25$ to $s = a$, the resulting patterns include hexagonal, cubic, and asymmetric defects. We note that the binding energy of similar impurities has recently been studied in a fermionic system [39]. In the antiparallel case, $d_B = -d_A$, the interlayer interaction is repulsive. This can be achieved using internal rotational degrees of freedom [8]. The defect patterns depicted in Fig. 1(e) include cubic, fivefold symmetric, and triangular symmetries reminiscent of vacancy defects with an effective volume that can be tuned by the layer separation.

In both cases the combined system is a mixture of effective defects and molecules reminiscent of a binary mixture of dipoles, a well-known glass-forming liquid in the classical regime [30,31]. We note that the antiparallel setup allows one to induce defects with fivefold symmetry which may allow one to implement a quantum system similar to the recently proposed classical spin liquid model [21].

Glass dynamics.—Below we study the relevant glass order parameters from the dynamics of the proposed setup after the quench. In the classical regime we use molecular dynamics simulations. In the quantum regime we employ the recently developed dynamical path integral methods, which have been applied to the glass transition in Ref. [34] (for details see the Supplemental Material [38]). We note that these methods include quantum effects but ignore the exchange statistics between the particles, and we are interested mainly in the transition from the classical phase to a phase where quantum fluctuations become important.

A glass phase is identified by a dramatic increase in the relaxation time which diverges with $\tau_r \propto \exp[-1/(T - T_g)]$, where T_g is the ideal glass temperature [19]. This corresponds to an extended plateau in the self-intermediate scattering function [19], a two-time correlation function defined as

$$F(k^*, \Delta t) = \frac{1}{N}\sum_j \langle e^{ik^*[\mathbf{r}_j(t) - \mathbf{r}_j(t+\Delta t)]}\rangle. \tag{3}$$

Here, angular brackets $\langle\cdot\rangle$ denote averages over many realizations of the experiment after the quench. The sum runs over all particles in both layers $N = N_A + N_B$, and $k^* = |\mathbf{k}^*|$ is the absolute value of the characteristic k vector of the coupled system corresponding to the first peak in the static structure factor $S(\mathbf{k}) = (1/N)\sum_i \sum_j \langle e^{-i\mathbf{k}[\mathbf{r}_i - \mathbf{r}_j]}\rangle$, where r is the distance in the xy plane. Note that Eq. (3) bears some similarity with the Fourier transform of the density-density correlation function; however, here the sum runs over individual particles at different times. In the path integral picture, the analogous order parameter to the classical case Eq. (3) reads as [34]

$$\Phi(k^*, \Delta t) = \frac{1}{N\hbar\beta} \int_0^{\hbar\beta} d\lambda \langle \rho^\dagger(t + \Delta t + i\lambda)\rho(t)\rangle. \quad (4)$$

Here, $\rho(\mathbf{k}, \Delta t) = \sum_j^N e^{i\mathbf{k}\mathbf{r}_j}$ and the integral runs over the imaginary path integral time. The semiclassical approximation allows one to follow the real time propagation of the path integral neglecting exchange [40].

A crucial dynamical characteristic of the glass phase is its deviation from the linear diffusion law. In particular, the local diffusion of individual particles is spatially heterogeneous, a characteristic of the glass phase known as *dynamical heterogeneity*. The local diffusion of particle j is $\Delta r_j(\Delta t) = \langle \mathbf{r}_j(t + \Delta t) - \mathbf{r}_j(t)\rangle$ and the mean squared displacements $\langle \Delta r^2(\Delta t)\rangle = 1/N \sum_i \Delta r_i^2(\Delta t)$. In the presence of quantum fluctuations the analogous measure in the path integral picture is the root mean squared displacement of the projections of the path integral with $\hat{r}_j(t) = (1/N\hbar\beta) \times \int_0^{\hbar\beta} d\lambda r_j(t + i\lambda)$ and $\Delta \hat{r}_j(\Delta t) = \langle \hat{\mathbf{r}}_j(t + \Delta t) - \hat{\mathbf{r}}_j(t)\rangle$.

The unique feature of the bilayer system of ultracold molecules is the possibility to study glassy dynamics in both the classical and quantum regimes, which are characterized by the dominance of thermal versus quantum fluctuations, respectively. This transition can be controlled by three tunable parameters: s representing the layer separation, the dimensionless temperature K, and the dipolar crystal parameter r_d. The case of large r_d corresponds to the classical limit where the glass transition can be studied by varying K with fixed r_d. The averaged root mean square displacement as a function of time is shown in Fig. 2(a). The dynamics does not follow the Einstein diffusion law $\langle \Delta r^2(\Delta t)\rangle \neq 2Dd\Delta t$ but develops a plateau for an effective K of the combined system smaller than $K < 0.02$. Figure 2(b) shows the relaxation dynamics $F(k^*, \Delta t)$ for a final layer separation $s = 0.5a$ in the classical regime. Both setups with parallel and antiparallel dipoles show a growing plateau and enter a glass phase.

Including quantum fluctuations the relaxation dynamics of the system changes considerably. Figure 2(c) depicts the relaxation dynamics $\Phi(k^*, \Delta t)$ calculated from a path integral simulation as a function of r_d at a fixed K. With increasing r_d, the dynamics approaches the glass dynamics from the molecular dynamics simulation ($r_d \to \infty$). Lowering r_d allows one to study the influence of quantum fluctuations in the glass phase. In the bilayer system one can also reach the glass phase by variation of the layer separation as shown in Fig. 2(d). Note that, in contrast to classical model systems of colloids [31], here the dynamics after the initial thermalization is that of an isolated system (microcanonical). However, this does not influence the long tail part in the relaxation [41].

Measurement of dynamical heterogenity.—One way to measure the anomalous diffusion as a glass feature is to consider a subensemble of polar molecules in a small spatial region (*marker molecules*), which are addressed with a laser and transferred to another internal (e.g., hyperfine) state [4]. The position of this molecular cloud at a later time can be measured with optical techniques. The ultimate tool for such position measurements will be provided by the molecular quantum gas microscope with single site resolution [42]. Dynamical heterogeneity can be measured as follows: We mark molecules in a small region with laser waist size $R_0 > a$. After the system evolves in time, the positions of the marker molecules are measured by the extension of the cloud of marker molecules given by the radius of gyration, $R_g^2 = 1/(2N^2)\sum_{i,j}(\mathbf{r}_i - \mathbf{r}_j)^2$. In a liquid a cloud of tagged particles spreads out linearly with time while in an amorphous solid it is constant, $R_g/R_0 = 1$. In both cases this is independent of the initial position of the maker molecules as the dynamics is spatially homogeneous. However, in the glass phase due to dynamical heterogeneity the scaling differs significantly depending on the initial position (see Fig. 3). As the initial size is known (R_0 from the laser waist), a series of single (destructive) measurements after time Δt allows one to distinguish a glass from liquid or amorphous solid (see Fig. 3). Note that the marker molecules are quantum mechanically distinguishable, which changes the dynamics in the deep quantum regime when exchange statistics is included, which is not relevant in the present case.

In conclusion, we have shown that a bilayer system of polar molecules can, with properly chosen parameters, exhibit a glass phase in a regime where quantum fluctuations are of the order of thermal fluctuations. Thus, ultracold ensembles of polar molecules can provide a tunable paradigmatic model system for classical and quantum glass physics, where theory and experiment can meet in a yet unexplored parameter regime of glass physics, providing, in particular, a stimulus for theoretical developments.

We thank K. Binder and M. Baranov for fruitful discussions. Work supported by the Austrian Science Fund (FWF): P 25454-N27, SFB FOQUS, Marie Curie Initial Training Network COHERENCE, and ERC Synergy Grant UQUAM.

*w.lechner@uibk.ac.at

[1] D. S. Jin and J. Ye, Chem. Rev. **112**, 4801 (2012), and references therein.
[2] L. D. Carr, D. DeMille, R. V. Krems, and J. Ye, New J. Phys. **11**, 055049 (2009).
[3] K.-K. Ni, S. Ospelkaus, M. H. G. de Miranda, A. Pe'er, B. Neyenhuis, J. J. Zirbel, S. Kotochigova, P. S. Julienne, D. S. Jin, and J. Ye, Science **322**, 231 (2008).
[4] S. Ospelkaus, K.-K. Ni, G. Quemener, B. Neyenhuis, D. Wang, M. H. G. de Miranda, J. L. Bohn, J. Ye, and D. S. Jin, Phys. Rev. Lett. **104**, 030402 (2010).
[5] B. Yan, S. A. Moses, B. Gadway, J. P. Covey, K. R. A. Hazzard, A. M. Rey, D. S. Jin, and J. Ye, Nature (London) **501**, 521 (2013).
[6] J. Deiglmayr, A. Grochola, M. Repp, K. Mörtlbauer, C. Glück, J. Lange, O. Dulieu, R. Wester, and M. Weidemüller, Phys. Rev. Lett. **101**, 133004 (2008).

[7] J. G. Danzl, E. Haller, M. Gustavsson, M. J. Mark, R. Hart, N. Bouloufa, O. Dulieu, H. Ritsch, and H.-C. Nägerl, Science **321**, 1062 (2008).

[8] M. A. Baranov, M. Dalmonte, G. Pupillo, and P. Zoller, Chem. Rev. **112**, 5012 (2012).

[9] T. Lahaye, C. Menotti, L. Santos, M. Lewenstein, and T. Pfau, Rep. Prog. Phys. **72**, 126401 (2009).

[10] H. P. Büchler, E. Demler, M. Lukin, A. Micheli, N. Prokof'ev, G. Pupillo, and P. Zoller, Phys. Rev. Lett. **98**, 060404 (2007).

[11] G. E. Astrakharchik, J. Boronat, I. L. Kurbakov, and Y. E. Lozovik, Phys. Rev. Lett. **98**, 060405 (2007).

[12] N. R. Cooper and G. V. Shlyapnikov, Phys. Rev. Lett. **103**, 155302 (2009).

[13] M. Lewenstein, A. Sanpera, and V. Ahufinger, *Ultracold Atoms in Optical Lattices: Simulating Quantum Many-Body Systems* (Oxford University Press, Oxford, England, 2012).

[14] G. Pupillo, A. Griessner, A. Micheli, M. Ortner, D.-W. Wang, and P. Zoller, Phys. Rev. Lett. **100**, 050402 (2008).

[15] D.-W. Wang, M. D. Lukin, and E. Demler, Phys. Rev. Lett. **97**, 180413 (2006).

[16] A. Pikovski, M. Klawunn, G. V. Shlyapnikov, and L. Santos, Phys. Rev. Lett. **105**, 215302 (2010).

[17] A. C. Potter, E. Berg, D.-W. Wang, B. I. Halperin, and E. Demler, Phys. Rev. Lett. **105**, 220406 (2010).

[18] M. Knap, E. Berg, M. Ganahl, and E. Demler, Phys. Rev. B **86**, 064501 (2012).

[19] K. Binder and W. Kob, *Glassy Materials and Disordered Solids* (World Scientific, London, 2011).

[20] P. G. Debenedetti and F. H. Stillinger, Nature (London) **410**, 259 (2001).

[21] H. Shintani and H. Tanaka, Nat. Phys. **2**, 200 (2006).

[22] For quantum glasses as a result of disorder, see T. Roscilde and J. I. Cirac, Phys. Rev. Lett. **98**, 190402 (2007); L. Sanchez-Palencia and M. Lewenstein, Nat. Phys. **6**, 87 (2010); S. Gopalakrishnan, B. L. Lev, and P. M. Goldbart, Phys. Rev. Lett. **107**, 277201 (2011).

[23] D. Chandler and J. Garrahan, Annu. Rev. Phys. Chem. **61**, 191 (2010).

[24] H. Tanaka, T. Kawasaki, H. Shintani, and K. Watanabe, Nat. Mater. **9**, 324 (2010).

[25] G. H. Fredrickson and H. C. Andersen, Phys. Rev. Lett. **53**, 1244 (1984).

[26] S. Whitelam, L. Berthier, and J. P. Garrahan, Phys. Rev. E **71**, 026128 (2005).

[27] B. Coluzzi, G. Parisi, and P. Verrocchio, Phys. Rev. Lett. **84**, 306 (2000).

[28] V. Lubchenko and P. G. Wolynes, Adv. Chem. Phys. **136**, 95 (2007).

[29] G. L. Hunter and E. R. Weeks, Rep. Prog. Phys. **75**, 066501 (2012).

[30] E. R. Weeks, J. C. Crocker, A. C. Levitt, A. Schofield, and D. A. Weitz, Science **287**, 627 (2000).

[31] F. Ebert, P. Keim, and G. Maret, Eur. Phys. J. E **26**, 161 (2008).

[32] V. N. Novikov and A. P. Sokolov, Phys. Rev. Lett. **110**, 065701 (2013).

[33] E. Rabani and D. R. Reichman, Annu. Rev. Phys. Chem. **56**, 157 (2005).

[34] T. E. Markland, J. A. Morrone, B. J. Berne, K. Miyazaki, E. Rabani, and D. R. Reichman, Nat. Phys. **7**, 134 (2011).

[35] T. E. Markland, J. A. Morrone, K. Miyazaki, B. J. Berne, D. R. Reichman, and E. Rabani, J. Chem. Phys. **136**, 074511 (2012).

[36] M. Boninsegni, L. Pollet, N. Prokof'ev, and B. Svistunov, Phys. Rev. Lett. **109**, 025302 (2012).

[37] M. Repp, R. Pires, J. Ulmanis, R. Heck, E. D. Kuhnle, M. Weidemüller, and E. Tiemann, Phys. Rev. A **87**, 010701 (2013); S.-K. Tung, C. Parker, J. Johansen, C. Chin, Y. Wang, and P. S. Julienne, Phys. Rev. A **87**, 010702 (2013).

[38] See Supplemental Material at http://link.aps.org/supplemental/10.1103/PhysRevLett.111.185306 for further numerical details.

[39] N. Matveeva and S. Giorgini, arXiv:1306.5588.

[40] M. Ceriotti, M. Parrinello, T. E. Markland, and D. E. Manolopoulos, J. Chem. Phys. **133**, 124104 (2010).

[41] T. Gleim, W. Kob, and K. Binder, Phys. Rev. Lett. **81**, 4404 (1998).

[42] J. Ye (private communication); For the atomic quantum gas microscope, see W. S. Bakr, J. I. Gillen, A. Peng, S. Fölling, and M. Greiner, Nature (London) **462**, 74 (2009); C. Weitenberg, M. Endres, J. F. Sherson, M. Cheneau, P. Schauß, T. Fukuhara, I. Bloch, and S. Kuhr, Nature (London) **471**, 319 (2011).